

---

# ON DISINTEGRATION OF LEAN HYDROGEN FLAMES IN NARROW GAPS

---

A PREPRINT

**Jorge Yanez\***

Institute for Thermal Energy Technology and Safety  
Karlsruhe Institute of Technology  
Hermann-von-Helmholtz-Platz, 1  
Karlsruhe, Germany.  
jorge.yanez@kit.edu

**Leonid Kagan**

School of Mathematical Sciences,  
Tel Aviv University  
Tel Aviv, Israel.  
kaganleo@tauex.tau.ac.il

**Mike Kuznetsov**

Institute for Thermal Energy Technology and Safety  
Karlsruhe Institute of Technology  
Hermann-von-Helmholtz-Platz, 1  
Karlsruhe, Germany.  
mike.kuznetsov@kit.edu

**Gregory Sivashinsky**

School of Mathematical Sciences,  
Tel Aviv University  
Tel Aviv, Israel.  
grishas@tauex.tau.ac.il

## ABSTRACT

The disintegration of near limit flames propagating through the gap of Hele-Shaw cells has recently become a subject of active research. In this paper, the flamelets resulting from the disintegration of the continuous front are interpreted in terms of the Zeldovich flame-balls stabilized by volumetric heat losses. A complicated free-boundary problem for 2D self-drifting near circular flamelets is reduced to a 1D model. The 1D formulation is then utilized to obtain the locus of the flamelet velocity, size, heat losses and Lewis numbers at which the self-drifting flamelets may exist.

**Keywords** Hydrogen flames · Diffusive-thermal instability · Flame-balls

---

\*Corresponding author

## 1 Introduction

Hydrogen flames have gained increasing attention over the last years as a clean and efficient energy solution [1]. Apart from their technological relevance, hydrogen flames are remarkably rich dynamically. Because of the high diffusion coefficient of molecular hydrogen, lean hydrogen-air flames are known to experience diffusive-thermal instability [2,3] manifesting themselves in the formation of a cellular structure in a state of chaotic self-motion. Moreover, as has recently been discovered by Veiga-López et al. [4], lean hydrogen-air flames evolving in narrow gaps of Hele-Shaw chambers, and where heat-loss effects become important, continuous cellular flames may disintegrate forming self-drifting cup-like flamelets leaving tree-like or sprout-like traces (Fig. 1).

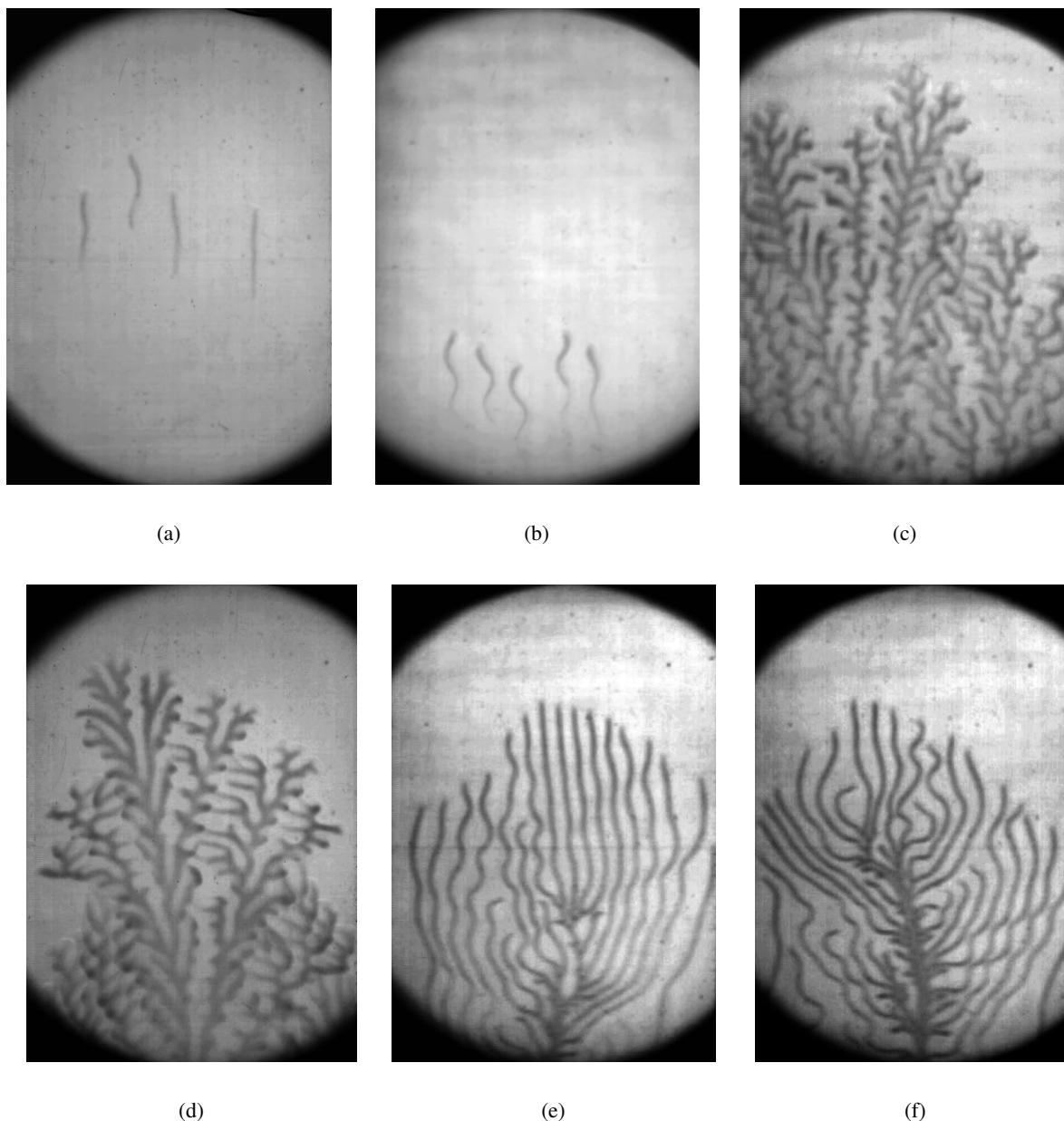


Figure 1: Hydrogen-air flamelets propagating through narrow gaps: (a)  $d = 5\text{mm}$ ,  $\%H_2 = 5.0$ ; (b)  $d = 3\text{mm}$ ,  $\%H_2 = 7.5$ ; (c)  $d = 4\text{mm}$ ,  $\%H_2 = 7.0$ ; (d)  $d = 5\text{mm}$ ,  $\%H_2 = 6.0$ ; (e)  $d = 2\text{mm}$ ,  $\%H_2 = 9.75$ ; (f)  $d = 2\text{mm}$ ,  $\%H_2 = 9.75$ . Regimes: (a)(b) one-headed finger, (c)(d)(e)(f) one-headed branching.

These unexpected propagation modes extend flammability limits beyond those of the planar flames. This is particularly important for the safety studies of hydrogen-powered devices [5] as it implies that hydrogen flames may propagate in gaps much narrower than initially anticipated.

## 2 Reaction-diffusion model

Some of the above features of the Hele-Shaw flames may be successfully captured by an ultra-simple constant-density, buoyancy-free, reaction-diffusion model [6]. In suitably scaled variables and parameters it reads,

$$\frac{\partial T}{\partial t} = \frac{\partial^2 T}{\partial x^2} + \frac{\partial^2 T}{\partial y^2} + (1 - \sigma)\Omega - q(T - \sigma), \quad (1)$$

$$\frac{\partial C}{\partial t} = \frac{1}{Le} \left( \frac{\partial^2 C}{\partial x^2} + \frac{\partial^2 C}{\partial y^2} \right) - \Omega, \quad (2)$$

$$\Omega = \frac{1}{2Le} (1 - \sigma)^2 N^2 C \exp \left[ N \left( 1 - \frac{1}{T} \right) \right], \quad (3)$$

where  $T$  = temperature in units of  $T_b$ , the adiabatic temperature of combustion products;  $C$  = concentration of the deficient reactant in units of  $C_0$ , its value in the fresh mixture;  $x, y, t$  = spatio-temporal coordinates in units of  $\ell_{th} = D_{th}/U_b$  and  $\ell_{th}/U_b$ , respectively;  $\ell_{th}$  = thermal width of the flame;  $U_b$  = speed of a planar adiabatic flame;  $D_{th}$  = thermal diffusivity of the mixture,  $\sigma = T_0/T_b$ , where  $T_0$  = temperature sustained at the walls of the Hele-Shaw cell;  $Le = D_{th}/D_{mol}$  is the Lewis number;  $D_{mol}$  = molecular diffusivity of the deficient reactant;  $N = T_a/T_b$  = scaled activation energy;  $T_a$  = activation temperature;  $\Omega$  = appropriately normalized reaction rate to ensure that at large  $N$  the scaled speed of the planar adiabatic flame is close to unity;  $q$  = scaled heat loss intensity specified as  $(\pi\ell_{th}/d)^2$ ;  $d$  = width of the Hele-shaw cell. The adopted expression for  $q$  stems from the 1D heat equation,  $T_t = T_{zz}$ , considered over the Hele-Shaw gap and subjected to isothermal boundary conditions,  $T(z = \pm d/2\ell_{th}, t) = \sigma$ . Hence,  $T - \sigma \sim \exp \left[ -(\pi\ell_{th}/d)^2 t \right] \cos [(\pi\ell_{th}/d) z]$ . The exponential rate of the temperature decay is then extrapolated over the quasi-2D formulation of (1)-(2) in the  $(x, y)$  plane.

Figures 2 and 3 display the results of numerical simulations of the effect of heat losses on the breaking up of the flame in 2D. The problem has also been explored by Martínez-Ruiz et al. [7] and Dejoan [8] through large-scale numerical simulations of a model accounting both for the gas thermal expansion, buoyancy and momentum loss.

Near the quenching point,  $q = 0.22$ , higher heat losses lead to a smaller drift velocity and flamelet size (Fig. 2), which is in line with experimental findings (Figs. 4, 5). Note that  $q = 0.22$  significantly exceeds the quenching point  $q = 0.018$  for the planar flame, other conditions being identical (Fig.6).

## 3 Reduction to a free-boundary problem

The fingering patterns of Figs.1-3 are traces of self-drifting near circular reactive spots. They may be regarded as a 2D version of familiar self-drifting 3D flame-balls [10, 11] (see also comment ii) of Sec. 5). This observation in turn suggests the possible existence of individual self-drifting 2D flame-balls described by time-independent reaction-diffusion equations,

$$V \frac{\partial T}{\partial \eta} = \frac{\partial^2 T}{\partial \xi^2} + \frac{\partial^2 T}{\partial \eta^2} + (1 - \sigma)\Omega - q(T - \sigma), \quad (4)$$

$$V \frac{\partial C}{\partial \eta} = \frac{1}{Le} \left( \frac{\partial^2 C}{\partial \xi^2} + \frac{\partial^2 C}{\partial \eta^2} \right) + (1 - \sigma)\Omega, \quad (5)$$

subjected to boundary conditions,

$$T(\xi^2 + \eta^2 \rightarrow \infty) = \sigma, \quad C(\xi^2 + \eta^2 \rightarrow \infty) = 1. \quad (6)$$

Here  $\xi = x$ ,  $\eta = y + Vt$ , and  $V$  is an eigen-value of the problem. For theoretical analysis it is technically advantageous to employ the familiar large-activation-energy ( $N \gg 1$ ) near-equidiffusive ( $Le^{-1} - 1 \ll 1$ ) approach where the reaction-diffusion system (4) and (5) is reduced to a free-boundary problem [12]. There, the reaction rate  $\Omega$  transforms into a localized source distributed along the interface  $\eta = R(\theta) \cos \theta$ ,  $\xi = R(\theta) \sin \theta$ . Eqs. (4) (5) translate into the

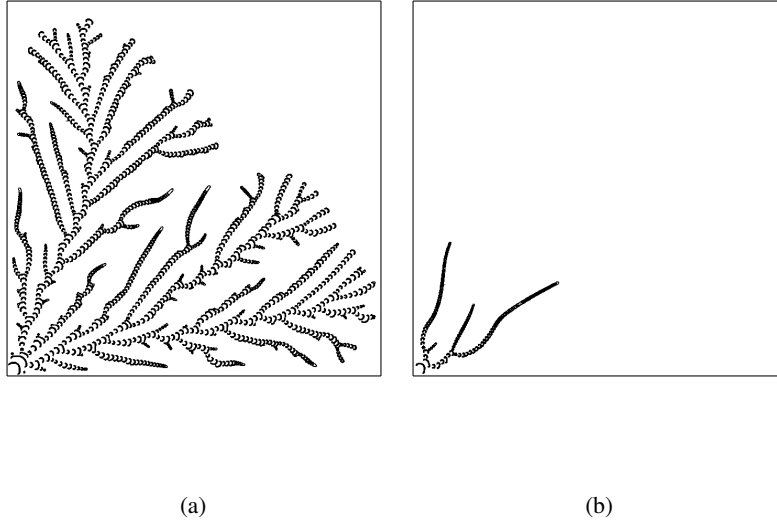


Figure 2: Reaction rate  $\Omega = 0.4$  at consecutive equispaced instants for one-headed flamelets under heat losses. Simulation of the reactive-diffusive system (1)-(3) for  $N = 10$ ;  $Le = 0.25$ ;  $\sigma = 0.2$ ;  $q = 0.14$ ,  $0 < t < 740$  (a);  $q = 0.20$ ,  $0 < t < 1000$  (b);  $0 < x, y < 480$ . Initial conditions,  $T(x, y, 0) = \sigma + (1 - \sigma) \exp[-(x^2 + y^2)/\ell^2]$ ,  $\ell = 0.25$ ,  $C(x, y, 0) = 1$ , and adiabatic boundary conditions.

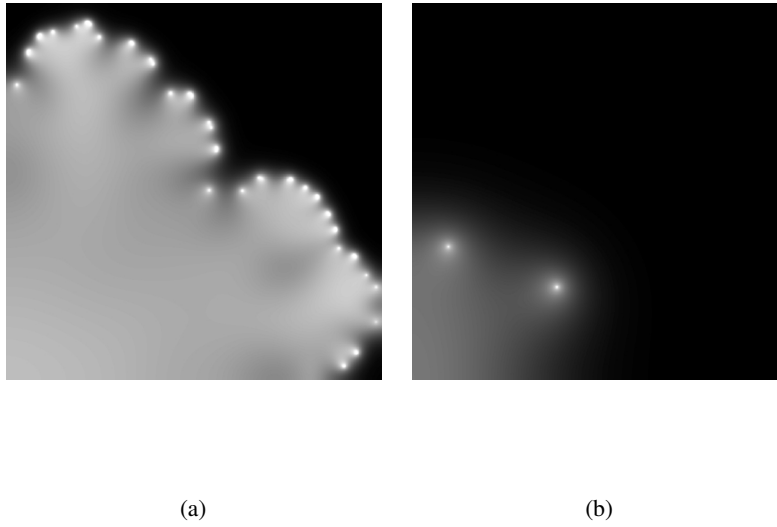


Figure 3: Distribution of the deficient reactant concentration,  $C$ , at  $t = 740$  (a) and  $t = 1000$  (b). For conditions see the legend for Fig.2. Lighter shading corresponds to lower concentration.

familiar set of equations for the reduced temperature  $\Theta$  and excess-enthalpy  $S$ ,

$$V \frac{\partial \Theta^{(0)}}{\partial \eta} = \frac{\partial^2 \Theta^{(0)}}{\partial \xi^2} + \frac{\partial^2 \Theta^{(0)}}{\partial \eta^2}, \quad (7)$$

$$V \frac{\partial S}{\partial \eta} = \frac{\partial^2 (S - \alpha \Theta^{(0)})}{\partial \xi^2} + \frac{\partial^2 (S - \alpha \Theta^{(0)})}{\partial \eta^2} - \nu \Theta^{(0)} \quad (8)$$

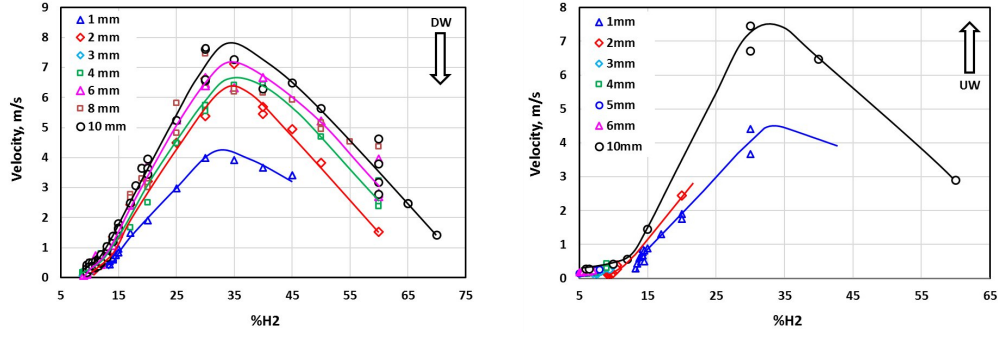


Figure 4: Drift velocity for downward (DW) and upward (UW) propagation. See also Kuznetsov et al. [9 Fig. 7]. The flame-ball regime corresponds to ultralean flames ( $\%H_2 < 20$ ).

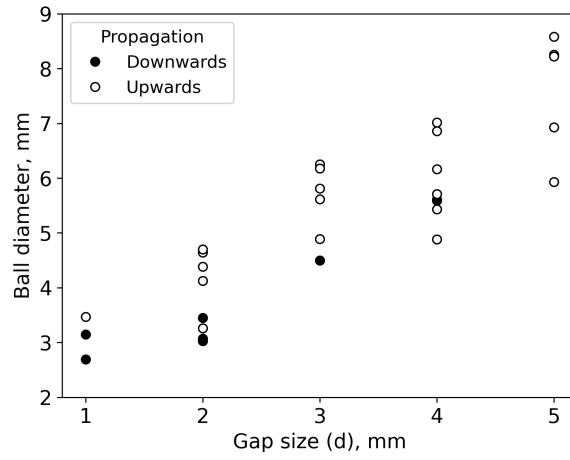


Figure 5: Flamelet diameter vs. gap size for one-headed flamelets.

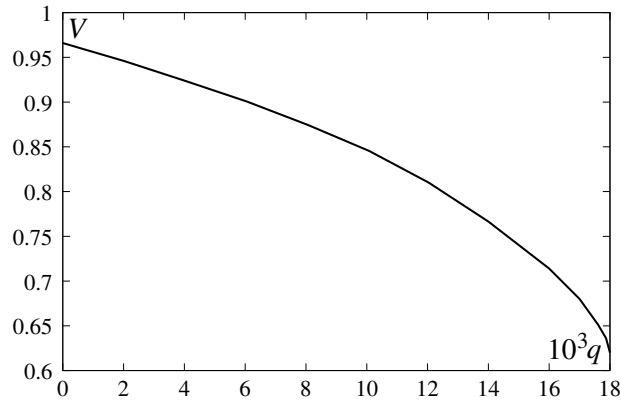


Figure 6: Drift velocity  $V$  vs. heat loss intensity  $q$  for a planar flame.

Here  $\Theta = (T - \sigma)/(1 - \sigma)$ ;  $S = (\Theta + C - 1)\beta$ ; the Zeldovich number  $\beta = (1 - \sigma)N$ , is assumed to be large;  $\alpha = (Le^{-1} - 1)\beta$ ,  $\nu = q\beta$  are assumed to be finite;  $\Theta^{(0)} = \Theta(\beta \rightarrow \infty)$ .

At the reactive interface,  $\xi^2 + \eta^2 = R^2(\theta)$ , the following conditions are held,

$$[S]_-^+ = 0, \quad \Theta^{(0)} = 1, \quad (9)$$

$$\left[ \frac{\partial S}{\partial n} \right]_-^+ = \alpha \left[ \frac{\partial \Theta^{(0)}}{\partial n} \right]_-^+, \quad (10)$$

$$\left[ \frac{\partial \Theta^{(0)}}{\partial n} \right]_-^+ = - \left( 1 + \frac{1}{R^2} \left( \frac{\partial R}{\partial \theta} \right)^2 \right)^{1/2} \exp \left( \frac{S}{2} \right). \quad (11)$$

Here  $\partial/\partial n$  is the normal derivative. And,

$$\Theta^{(0)} \rightarrow 0, \quad S \rightarrow 0, \quad (12)$$

at  $\xi^2 + \eta^2 \rightarrow \infty$ . Within the flame-ball interface the deficient reactant is assumed to be fully consumed,

$$C(\xi^2 + \eta^2 \leq R^2(\theta)) = 0. \quad (13)$$

Finally we observe that Eq. (7) allows for the exact solution which in polar coordinates ( $\eta = r \cos \theta$ ,  $\xi = r \sin \theta$ ) reads, [13, 14],

$$\begin{aligned} \Theta^{(0)}(r, \theta) = & \sum_m \exp(kr \cos \theta) \cos(m\theta) \cdot \\ & \cdot [A_m K_m(kr) + B_m I_m(kr)] + H. \end{aligned} \quad (14)$$

Here  $K_m, I_m$  are modified Bessel functions of first and second kind,  $k = V/2$ , and  $A_m, B_m, H$  are parameters to be determined by conditions at  $r = 0$ ,  $r = \infty$  and  $r = R(\theta)$ .

## 4 Reduction to a 1D model

### 4.1 General

The 2D free-boundary problem (7) - (13) is still too difficult for a straightforward analytical treatment. We therefore propose to consider its low-mode allocation-like reduction to a 1D model that we believe will keep enough contact with the original 2D formulation. More specifically, in the 1D approach  $\Theta, C, S$  are projected on the  $\eta$ -axis running through the center of the flame ball (Fig. 7). There the interior of the flame-ball covers the interval  $-R < \eta < R$ . In

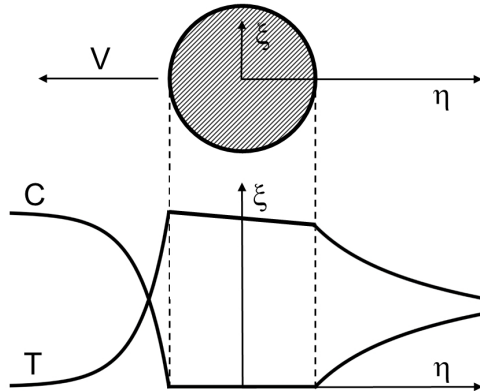


Figure 7: Up: Top sketch view of the flamelet in a plane parallel both to the paper and to the plates of the Hele-Shaw cell. Down: Profiles of temperature,  $T$ , and concentration,  $C$ , through the center of the flame-ball.

the expansion (14) we will keep only the leading order terms corresponding to  $m = 0$ . Moreover, we will set  $\theta = 0$  for

$\eta > 0$  and  $\theta = \pi$  for  $\eta < 0$ . Conditions (9) - (13) on the flame-ball interface  $\eta = \pm R$  and  $\eta = \pm\infty$  thus become,

$$[S]_{\pm}^+ = 0, \quad \Theta^{(0)} = 1, \quad (15)$$

$$\left[ \frac{\partial \Theta^{(0)}}{\partial \eta} \right]_{\pm}^+ + \exp\left(\frac{S}{2}\right) = 0, \quad (16)$$

$$\left[ \frac{\partial S}{\partial \eta} \right]_{\pm}^+ = \alpha \left[ \frac{\partial \Theta^{(0)}}{\partial \eta} \right]_{\pm}^+, \quad (17)$$

$$\Theta^{(0)}(\eta = \pm\infty) = 0, \quad S(\eta = \pm\infty) = 0. \quad (18)$$

And

$$C(-R < \eta < R) = 0. \quad (19)$$

For the leading order approximation,  $\beta \gg 1$ ,

$$\Theta^{(0)}(\eta > R) = \exp[k(\eta - R)] \frac{K_0(k\eta)}{K_0(kR)}, \quad (20)$$

$$\Theta^{(0)}(\eta < -R) = \exp[k(\eta + R)] \frac{K_0(-k\eta)}{K_0(kR)}, \quad (21)$$

$$\Theta^{(0)}(-R < \eta < R) = 1, \quad (22)$$

$$C^{(0)}(\eta) = 1 - \Theta^{(0)}(\eta). \quad (23)$$

For the higher order uniform approximation needed for evaluation of  $S = (\Theta + C - 1)\beta$ ,

$$\begin{aligned} \Theta(\eta > R) &= [1 + \beta^{-1}S(R)] \cdot \\ &\cdot \exp[k(\eta - R)] \frac{K_0\left((k^2 + q)^{\frac{1}{2}}\eta\right)}{K_0\left((k^2 + q)^{\frac{1}{2}}R\right)}, \end{aligned} \quad (24)$$

$$\begin{aligned} \Theta(\eta < -R) &= [1 + \beta^{-1}S(-R)] \cdot \\ &\cdot \exp[k(\eta + R)] \frac{K_0\left(-\left(k^2 + q\right)^{\frac{1}{2}}\eta\right)}{K_0\left(\left(k^2 + q\right)^{\frac{1}{2}}R\right)}, \end{aligned} \quad (25)$$

$$\Theta(-R < \eta < R) = 1 + \beta^{-1}S(-R < \eta < R), \quad (26)$$

$$\begin{aligned} S(-R < \eta < R) &= A + B \exp(k\eta) I_0(k|\eta|) \\ &\quad - \nu\eta/2k, \end{aligned} \quad (27)$$

where,

$$\begin{aligned} A &= [S(R) + S(-R)] \\ &\quad - \frac{1}{2}BI_0(kR) [\exp(kR) + \exp(-kR)] \end{aligned} \quad (28)$$

$$B = \frac{\nu R + S(R) - S(-R)}{kI_0(kR) [\exp(kR) - \exp(-kR)]}, \quad (29)$$

$$C(\eta > R) = 1 - \exp[kLe(\eta - R)] \frac{K_0(kLe\eta)}{K_0(kLeR)}, \quad (30)$$

$$C(\eta < -R) = 1 - \exp[kLe(\eta + R)] \frac{K_0(-kLe\eta)}{K_0(kLeR)}, \quad (31)$$

$$C(-R < \eta < R) = 0. \quad (32)$$

The uniform approximation employed in the above equations allows meeting the boundary conditions  $\Theta(\eta \rightarrow \infty) = 0$ ,  $S(\eta \rightarrow \infty) = 0$ , behind the self-drifting flamelet, where  $\eta \sim \beta$ .

## 4.2 Results

Eqs. (20) - (32) meet the continuity conditions (15) at  $\eta = \pm R$ . Substituting Eqs. (20) - (32) into jump conditions (16), (17) one ends up with four algebraic relations for four unknown parameters  $V = 2k$ ,  $R$ ,  $S(R)$ ,  $S(-R)$  as functions of  $\alpha$ ,  $\nu$ ,  $\beta$  (Figs. 8, 9, 10). More technical details and the numerical procedure employed for the emerging algebraic problem are presented in the earlier version of the paper [15].

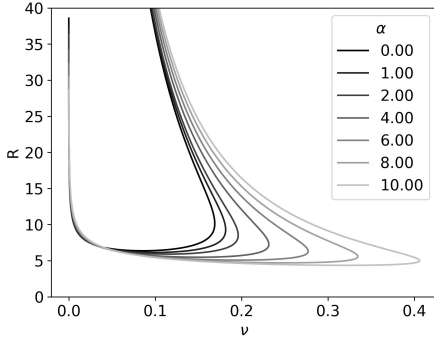


Figure 8: Locus of the flamelet radii,  $R$ , as a function of the heat losses,  $\nu$ , for different Lewis number parameters,  $\alpha$ .

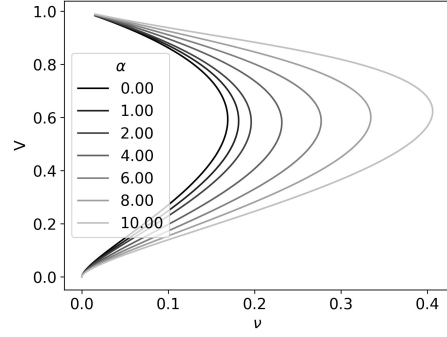


Figure 9: Locus of the velocities,  $V$ , as a function of the heat losses,  $\nu$ , for different Lewis number parameters,  $\alpha$ .

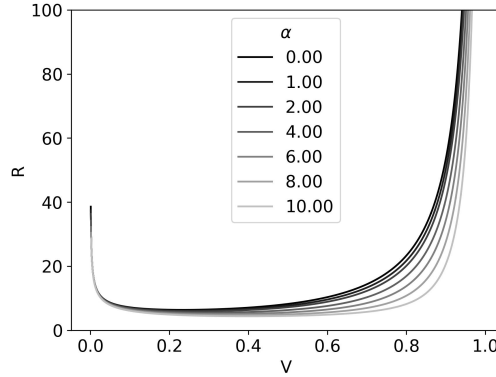


Figure 10: Locus of the flamelet radii,  $R$ , as a function of velocity,  $V$ , for different Lewis number parameters,  $\alpha$ .

One can draw several conclusions from the results obtained.

- Parameter  $\alpha$  strongly affects  $V(\nu)$ ,  $R(\nu)$  - dependencies. The heat loss intensity at the quenching (turning) point,  $\nu_q$ , increases with the decrease of the Lewis number,  $Le \simeq 1 - \alpha/\beta$ .
- At  $\nu < \nu_q$  the multiplicity of  $V(\nu)$ ,  $R(\nu)$  is observed. A similar non-uniqueness is known to occur in planar ( $R = \infty$ ) non-adiabatic flames which leads to the  $\alpha$ -independent relation between  $V$  and  $\nu$ ,  $V^2 \ln(1/V) = \nu$ , [16].
- Once the solutions for  $V(\nu)$ ,  $R(\nu)$  for a certain  $\alpha$  are available, one can plot spatial profiles of all state variables involved. For brevity we depict here only  $\Theta(\eta)$  for the upper and lower branches of  $V(\eta)$  (Figs. 11, 12). A significant drop of temperature  $\Theta$  at the rear side ( $\eta = R$ ) of the self-drifting flame-ball might explain the horseshoe shape of the advancing flamelet. The latter is often perceived as a local extinction (opening) of the front.



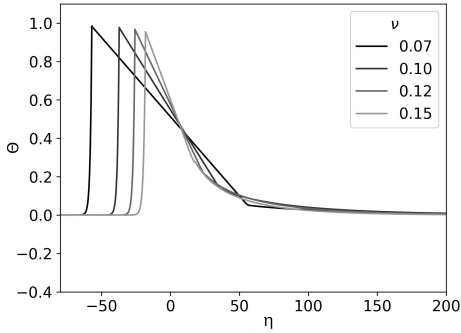


Figure 11: Profiles of  $\Theta$  for  $\alpha = 1$ ,  $\beta = 10$  and different values of  $\nu$  for the upper branch of  $V(\nu)$ .

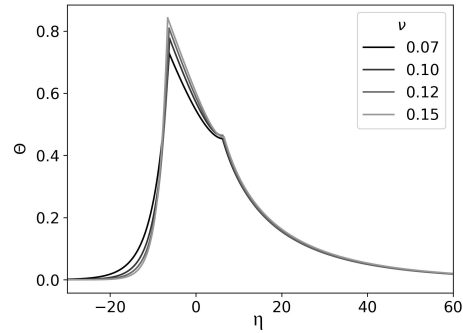


Figure 12: Profiles of  $\Theta$  for  $\alpha = 1$ ,  $\beta = 10$  and different values of  $\nu$  for the lower branch of  $V(\nu)$ .

## 5 Concluding remarks

- (i) In constructing a workable approximate solution we truncated the series involving an infinite number of terms, as in Eq. (14), setting  $m$  at zero, to deal with sums involving only a finite number of terms.
- (ii) There is an important distinction between the 3D and effectively 2D situation typical of large aspect ratio Hele-Shaw cells. The 3D case allows for stationary spherical flame-balls which may bifurcate into a self-drifting mode [10, 11]. In the 2D case, the non-drifting circular flame-balls are ruled out. They cannot meet boundary conditions at infinity (due to the logarithmic tail of the associated concentration profiles [7]). So, in narrow gaps 2D self-drifting flame-balls should emerge not as a bifurcation but rather as the only way for the 2D flame-balls to exist.
- (iii) In the present study the pattern of the flame disintegration is controlled by the heat loss intensity  $q = (\pi \ell_{th}/d)^2$ , which in turn may be controlled by the width of the Hele-Shaw gap ( $d$ ) or the mixture composition ( $\% H_2$  or  $\ell_{th}$ ) [4, 9, 17].
- (iv) The reaction-diffusion model of Sec. 2 does not seem capable of reproducing two-headed flamelets. The latter is often observed experimentally [4, 18] as well as in simulations of more sophisticated models that consider the burned gas thermal expansion [7, 19] and are therefore susceptible to Darrieus-Landau instability. At the moment the issue of two-headed flamelets remains unexplained.
- (v) The present work is devoted to estimates of the propagation velocity of an individual flame-ball in a flat channel. It would be interesting to extend the analysis over the collective propagation of a group of flame-balls appearing in Figs. 1-3, and where the flamelets are competing for common fuel and mutual heating of one another. A mean-field type of approach as the developed by D'Angelo and Joulin [20] or Williams and Grcar [21] seems particularly promising.
- (vi) In the present study flame-balls emerge in gaseous premixtures as an extreme case of diffusive-thermal instability where invariably  $Le < 1$ . A similar pattern is observed in smoldering burning of thin solid sheets with and without imposed air flows [22-28]. There, similar to the gaseous systems, the effective Lewis number is considerably below unity [28]. It would be interesting to extend the 1D approach of this paper also to the smoldering problem.

### Declaration of competing interest

The authors declare that they have no known competing financial interests or personal relationships that could have appeared to influence the work reported in this paper.

### Acknowledgements

This research was supported in part by the US-Israel Binational Science Foundation (Grant 2020-005).

## References

- [1] E.-A. Tingas, A. M. K. P. Taylor, Hydrogen for future thermal engines, Springer, 2023.

- [2] F. A. Williams, *Combustion theory*, Perseus Book Pub., Reading, Massachusetts, 1985.
- [3] P. Clavin, G. Searby, *Combustion waves and fronts in flows: flames, shocks, detonations, ablation fronts and explosion of stars*, Cambridge University Press, 2016.
- [4] F. Veiga-López, M. Kuznetsov, D. Martínez-Ruiz, E. Fernández-Tarrazo, J. Grune, M. Sánchez-Sanz, Unexpected propagation of ultra-lean hydrogen flames in narrow gaps, *Phys. Rev. Lett.* 124 (2020) 174501.
- [5] M. Kuznetsov, J. Grune, Experiments on combustion regimes for hydrogen/air mixtures in a thin layer geometry, *International Journal of Hydrogen Energy* 44 (17) (2019) 8727–8742.
- [6] L. Kagan, G. Sivashinsky, Self-fragmentation of nonadiabatic cellular flames, *Combust. Flame* 108 (1997) 220–226.
- [7] D. Martínez-Ruiz, F. Veiga-López, D. Fernández-Galisteo, V. N. Kurdyumov, M. Sánchez-Sanz, The role of conductive heat losses on the formation of isolated flame cells in Hele-Shaw chambers, *Combust. Flame* 209 (2019) 187–199.
- [8] A. Dejoan, D. Fernández-Galisteo, V. N. Kurdyumov, Numerical study of the propagation patterns of lean hydrogen-air flames under confinement, 29th ICDERS, July 23-28, SNU Siheung, Korea, 2023.
- [9] M. Kuznetsov, J. Yanez, F. Veiga-López, Near limit flame propagation in a thin layer geometry at low Peclet numbers, in: *Proc. 18th Int. Conference on Flow Dynamics (ICFD 2021)*, no. OS18-8, 2022, pp. 688–692.
- [10] I. Brailovsky, G. Sivashinsky, On stationary and travelling flame balls, *Combust. Flame* 110 (1997) 524–529.
- [11] S. Minaev, L. Kagan, G. Joulin, G. Sivashinsky, On self-drifting flame balls, *Combust. Theor. Model.* 5 (2001) 609.
- [12] B. Matkowsky, G. Sivashinsky, An asymptotic derivation of two models in flame theory associated with the constant density approximation, *SIAM J. App. Math.* 37 (1979) 686–699.
- [13] H. Lamb, *Hydrodynamics*, Cambridge University Press, 1924.
- [14] S. Tomotika, T. Aoi, The steady flow of viscous fluid past a sphere and circular cylinder at small Reynolds numbers, *Q. J. Mech. Appl. Math.* 3 (1950) 141–161.
- [15] J. Yanez, L. Kagan, G. Sivashinsky, M. Kuznetsov, Modeling of 2D self-drifting flame-balls in Hele-Shaw cells, *Combustion and Flame* 258 (2023) 113059.
- [16] G. Sivashinsky, B. Matkowsky, On the stability of nonadiabatic flames, *SIAM Journal on Applied Mathematics* 40 (2) (1981) 255–260.
- [17] P. V. Moskalev, V. P. Denisenko, I. A. Kirillov, Classification and dynamics of ultralean hydrogen-air flames in horizontal cylindrical Hele-Shaw cells, *Journal of Experimental and Theoretical Physics* 137 (1) (2023) 104–113.
- [18] J. Y. Escanciano, M. Kuznetsov, F. Veiga-López, Characterization of unconventional hydrogen flame propagation in narrow gaps, *Phys. Rev. E* 103 (2021) 033101.
- [19] A. Domínguez-González, D. Martínez-Ruiz, M. Sánchez-Sanz, Stable circular and double-cell lean hydrogen-air premixed flames in quasi twodimensional channels, *Proc. Combust. Inst.* (2022).
- [20] Y. D’Angelo, G. Joulin, Collective effects and dynamics of non-adiabatic flame balls, *Combustion Theory and Modelling* 5 (1) (2001) 1.
- [21] F. A. Williams, J. F. Grear, A hypothetical burning velocity formula for very lean hydrogen-air mixtures, *Proc. Combust. Inst.* 32 (1) (2009) 1351–1357.
- [22] Y. Zhang, P. Ronney, E. Roegner, J. Greenberg, Lewis number effects on flame spreading over thin solid fuels, *Combust. Flame* 90 (1992) 71–83.
- [23] O. Zik, Z. Olami, E. Moses, Fingering instability in combustion, *Phys. Rev. Lett.* 81 (1998) 3868.
- [24] T. Matsuoka, K. Nakashima, Y. Nakamura, S. Noda, Appearance of flamelets spreading over thermally thick fuel, *Proc. Combust. Inst.* 36 (2017) 3019–3026.
- [25] F. Zhu, Z. Lu, S. Wang, Y. Yin, Microgravity diffusion flame spread over a thick solid in step-changed low velocity opposed flows, *Combust. Flame* 205 (2019) 55–67.
- [26] J. Malchi, R. Yetter, S. Son, G. Risha, Nano-aluminum flame spread with fingering combustion instabilities, *Proc. Combust. Inst.* 31 (2) (2007) 2617–2624.
- [27] S. Olson, H. Baum, T. Kashiwagi, Finger-like smoldering over thin cellulosic sheets in microgravity, in: *Symp. (Int.) Combust.*, Vol. 27, Elsevier, 1998, pp. 2525–2533.
- [28] Y. Uchida, K. Kuwana, G. Kushida, Experimental validation of Lewis number and convection effects on the smoldering combustion of a thin solid in a narrow space, *Combust. Flame* 162 (5) (2015) 1957–1963.